Commun. Comput. Chem.
doi: 10.4208/cicc.2013.v1.n1.9

Vol.**1**, No.1, pp.88-98
January 2013

REGULAR ARTICLE

Time-Dependent Density Functional Theory Study on a Fluorescent Chemosensor Based on C–H···F Hydrogen-Bond Interaction

Guang-Yue Li[1,*], Yue-Hua Li[1], Hang Zhang[2], Guang-Hua Cui[1]

[1] *College of Chemical Engineering, Hebei United University, Tangshan, China, P. R. 063009*

[2] *Modern Technology and Education Centre, Hebei United University, Tangshan, China, P. R. 063009*

Received 14 December 2012; Accepted (in revised version) 22 January 2013

Special Issue: Guo-Zhong He Festschrift

Abstract: A new fluorescent chemosensor bearing two imidazolium groups was designed and investigated by DFT/TDDFT method. The fluoride-sensing mechanism of the chemosensor was studied by the geometry optimization, two-dimensional potential energy surface (PES) scan, absorption/emission spectra simulation, and frontier molecular orbital (FMO) analysis. The calculations show that this chemosensor displays an emission band at 407 nm. PES scan confirmed that the excited state proton transfer (ESPT) process of the chemosensor-fluoride complex is barrierless. The ESPT process took place in the C–H•••F hydrogen bond with C–H moiety acting as a proton donor and the fluoride anion acting as a proton acceptor. This process proved that addition of fluoride anion could lead to the formation of the carbene form of the chemosensor. Due to the nπ-type transition mode obtained by FMO, the carbene form has a red-shift emission band at 523 nm.

AMS subject classifications: 65D18, 68U05, 68U07

Key words: Chemosensor, Hydrogen bond, TDDFT, ESPT, Fluorescence

* Corresponding author. *Email address*: gyli@heuu.edu.cn (Guang-Yue Li)

1 Introduction

Hydrogen bond (H-bond) occurs in both inorganic molecules [1] and organic molecules. Especially, it plays a key role in determining the three-dimensional structures of proteins [2] and DNAs [3]. In these macromolecules, the H-bond between parts of the same macromolecule causes it to fold into a specific shape, which helps the molecule determine its biochemical role. According to the definition from IUPAC, H-bond is an attractive interaction between a hydrogen atom from an X–H group (H-bond donor) and an atom or a group with high electron density (H-bond acceptor) [4]. The X atom in H-bond donor or H-bond acceptor is always an electronegative atom, such as N, O, or F. So H-bonds involved N, O, or F are most frequently studied [5-7]. For some time there were researches on C–H moieties with electron-withdrawing groups, which were proved to be able to act as H-bond donors [8]. This is because the electron-withdrawing moieties lead to the electron pair in C–H moiety close to the carbon atom.

Due to the fundamental roles that anions play in a wide range of chemical and biological processes，numerous efforts have been devoted to the design of chemosensors capable of selectively sensing anions. The development of selective sensors for fluoride anions is of particular interest because they play vital roles in a wide range of our life，such as food science, dental care, and the treatment of osteoporosis [9-11]. midazolium cation can be formed by protonation or substitution at nitrogen atom of imidazole. It has been used as ionic liquids and precursors to stable carbenes [12]. As mentioned above, the C–H moiety between two nitrogen atoms in imidazolium cation is likely to form H-bond with electronegative atoms or anions [13-16]. The H-bond could be strengthened or weakened upon excitation [17-19] and can be monitored by fluorescent spectra. Accordingly, we can design a fluorescent chemosensor for fluoride anions. In general, free imidazolium do not have visible light absorption [20-23]. To improve the photoabsorption properties of imidazolium cations, some groups with conjugated structures can be introduced into the imidazolium skeleton [24,25]. Thus, the fluoride anion can be easily discerned by virtue of the distinct fluorescence wavelengths that they elicit.

Based on C–H•••F H-bond interaction, we designed a fluorescent chemosensor for fluoride anion, 1,1′-butane-1,4-diylbis(3-methylbenzimidazolium), (see **Figure 1**, abbreviated as b). This chemosensor can be easily synthesized by methylation of corresponding imidazole compound that is only slightly soluble in water. Forming imidazolium cation could increase the solubility of the chemosensor, which is favorable to sense the fluoride anions in aqueous solutions. The quantum-chemical calculations are performed to investigate molecular spectra and the structural parameters of the molecule. The

fluoride-sensing mechanism can be explained in details by this means. The mechanism is important for the design and synthesis of the fluorescent chemosensor. Further research on synthesis of this chemosensor is underway in our lab.

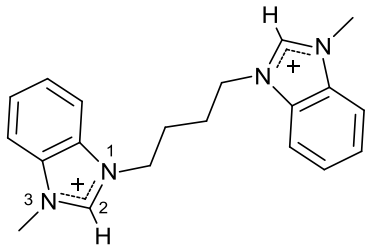

Figure 1: Structure of chemosensor **b**.

2 Computational Details

All calculations on electronic structures were carried out using the ORCA 2.8 program [26]. Geometry optimizations for the ground state and the first singlet electronic excited state of the chemosensor were performed using the density functional theory (DFT) and time-dependent density functional theory (TDDFT), respectively. B3P86 functional [27-30], Becke's three-parameter hybrid exchange functional with the non-local correlation provided by Perdew 86, was the more reasonable choice to be in good accordance with the experimental results and not time-consumption [31,32]. Then it was used in both the DFT and TDDFT methods in the sequential work. The triple-valence quality with one set of polarization functions (TZVP) [33] was chosen as basis sets throughout, which is an appropriate basis set for such ionic organic compounds. No constrains for symmetry, bonds, angles, or dihedral angles were applied in the geometry optimization calculations. To evaluate the solvent effect in the sensing process, water was employed as solvent in the SCRF calculations by using the conductor-like screening model (COSMO) method [34]. All of the local minima were confirmed by the absence of an imaginary mode in vibrational analysis calculations.

3. Results and Discussion

In our calculations we have started with structural optimizations of the chemosensor **b**, its fluoride complex (**bf**) and deprotonated structure (carbene form, **bc**) in the ground (S_0) state. The structural optimizations have been done on the B3P86 level and within the TZVP basis set. We find that all the three molecules converge to the C_i symmetry. The structures of the

investigated molecules are shown in **Figure 2**. In chemosensor **b**, the C2–H bond length is 1.097 Å. But in **bf**, the C2–H bond length is slightly elongated to 1.171 Å. Moreover, the calculated distance between H and F in **bf** is 1.627 Å, which is much longer than the length of the HF molecule (0.92 Å) [35].The C2–H and H–F bond lengths, as well as the C2–H–F bond angle (160.7º), indicate the formation of an intramolecular H-bond (C2–H–F). In **bf**, both the N1–C2 and C2–N3 bond lengths are 1.352 Å, and the N1–C2–N3 bond angle is 108.2º. In comparison with bc, the N1–C2 and C2–N3 bond lengths are respectively 1.368 Å and 1.369 Å, and the N1–C2–N3 bond angle is 103.4º. It is noted that **bf** exhibits almost the same geometric structure as **b**. The two molecules are expected to show similar photophysical and chemical properties.

Figure 3 presents the optical absorption spectra calculated with TDDFT/B3LYP approach. The red, blue and olive colors correspond to **b, bf** and **bc** in aqueous solutions, respectively. The continuous lines simulate the absorption spectra from the oscillator strengths of the electronic transitions between the S_0 and the first singlet excited (S_1) states, where relevant bands are approximated by the Lorentz function with the parameter of the full width at half maximum 0.25 eV. The strongest absorption band of **b** in the UV-region centered at about 272 nm. As predicted in geometry optimizations, the absorption spectrum of bf should be similar with **b**. In **Figure 3**, the absorption maximum of **bf** is only blue-shifted 7 nm in comparison with **b**. However, **bc** shows two main absorption bands, 295 and 355 nm. It indicates that **bc** could have different absorption mode from **b** or **bf.**

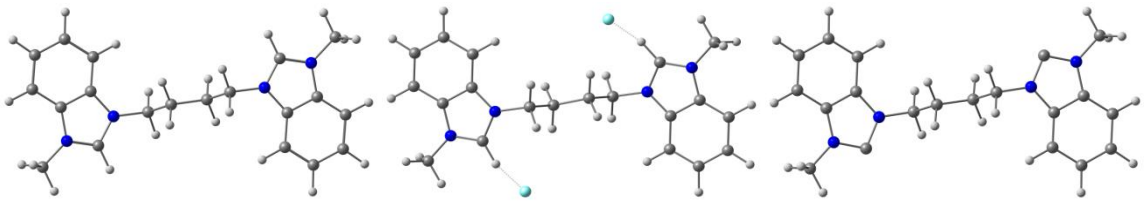

Figure 2: Optimized geometries of chemosensor **b**, **bf** and **bc** at the S_0 state. (gray: C; white: H; blue: N; cyan: F)

Frontier molecular orbital (FMO) theory has recently provided an elegant explanation for the electron process in the absorption spectra [36]. In this theory, the lowest unoccupied molecular orbital (LUMO) and the highest occupied molecular orbital (HOMO) play vital roles. As seen in **Figure 4**, both HOMO and LUMO of **b** are doubly degenerate, and they are delocalized over the benzimidazolium moiety. The orbital shapes show that the maximum absorption intensity of b is a dominant $\pi\pi$-type transition from HOMOs to LUMOs. In the case of **bc**, the HOMO and LUMO are also doubly degenerate. The HOMOs of **bc** are mainly

composed of the atomic orbital on the C2, which are nonbonding orbitals including lone electron pairs. So the maximum absorption intensity of **bc** is an nπ-type transition from HOMOs to LUMOs. The energy of the nonbonding orbital (n orbital in **Figure 5**) is higher than that of the bonding orbitals in **bc**. As a consequence, we can explain that the red shift of the maximum absorption band of **bc** in the calculated absorption spectra. It may be deduced that there will be obvious difference between the emission spectra of **b** and **bc**.

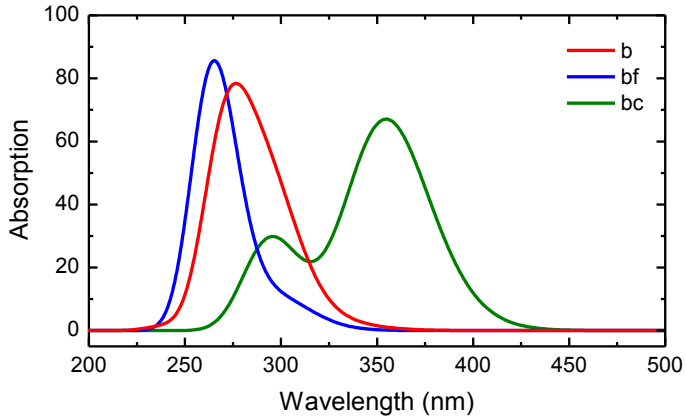

Figure 3: Calculated absorption spectra of **b, bf** and **bc**.

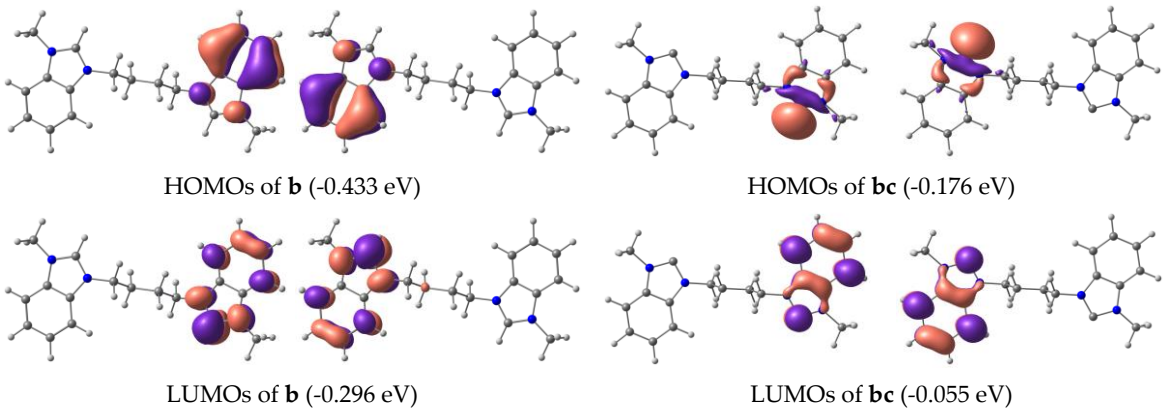

Figure 4: Frontier molecular orbitals shapes of **b** and **bc**.

The geometries of the S_1 states of **b**, **bf** and **bc** were optimized at the TDDFT/B3P86 /TZVP level of theory. The COSMO salvation model was used to evaluate the solvent effect of water. For the S_1 optimization process of three molecules, we used the initial

configurations obtained from the S_0 optimized geometries. The results of **b** and **bc** showed similar structures. For **bf**, the C2–H bond is shortened to 1.171 Å and the H–F bond is lengthened to 1.627 Å compared with its S_0 state. The transfer of the proton from C2 to F is energetically favorable for **bf** in the S_1 state. In order to confirm this process, the potential energy surface (PES) for the excited state proton transfer (ESPT) in **bf** is constructed and the results are displayed in **Figure 6**. In the PES, energy variation has been observed simultaneously as a function of the reaction coordinates C2–H and H–F distances. The S_1 surface reveals a barrierless way for the ESPT process (white arrows in **Figure 6**). In this process the H–F bond is shortened and the C2–H bond is lengthened. So, we surmise that there is the ESPT process from C2 to the F for the fluoride complex **bf**.

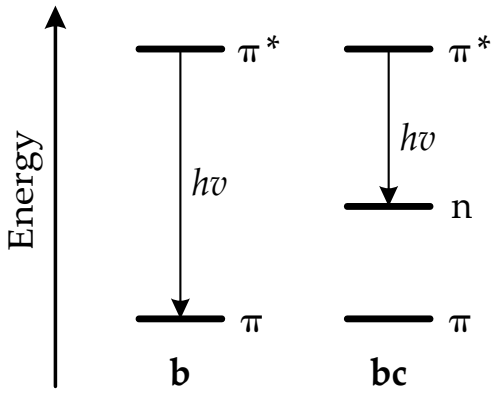

Figure 5: Energy levels of frontier molecular orbitals of **b** and **bc.**

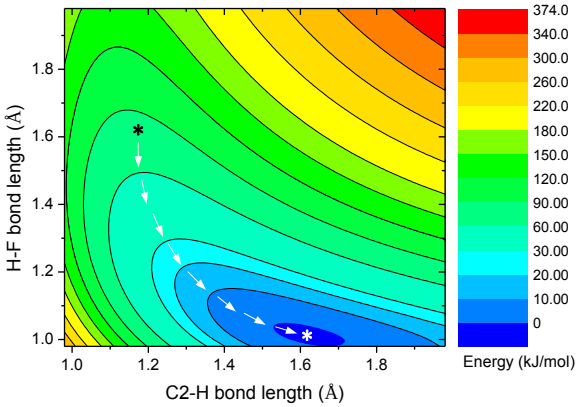

Figure 6: PES for the ESPT process of **bf**. (The black and white asterisks respectively refer to the S_0 and S_1 optimized geometries of **bf**.)

The S_1–S_0 vertical excitation energies of **b** and **bc** were simultaneously calculated to estimate their emission spectra (see **Figure 7**). For both **b** and **bc**, it is observed that, after relaxation to their S_1 state, the energies of the first electronic transitions decrease significantly. The chemosensor **b** displays an emission band with a maximum at 407 nm. For **bc**, this band is red-shifted to 523 nm. It can clearly be observed that the emission wavelength of **bc** are much longer than that of **b**. The emission wavelength difference of **b** and **bc** could be easily observed in the fluorescence spectra.

The results we presented confirm the fluoride-sensing mechanism of the designed fluorescence chemosensor **b**. **Figure 8** provides the detailed information of the sensing mechanism. In the S_0 state, the the C2–H moiety of **b** can capture the fluoride anion to form an H-bond. The fluoride complex **bf** absorbs the photon with a proper wavenumber, and is

excited to the S_1 state. At the same time, the C2–H bond is weakened and the H–F bond is strengthened by the electronic excitation. As reported, intermolecular H-bond strengthening and weakening could lead to red-shifts and blue-shifts in the electronic spectra [17–19]. ESPT takes place in **bf**, with C2–H moiety acting as a proton donor and the fluoride anion acting as a proton acceptor. Thus, **bf** in the S_1 state can be seen as **bc** binding a HF molecule. It could easily lose the HF molecule to form the carbene **bc**, whose emission band is red-shifted.

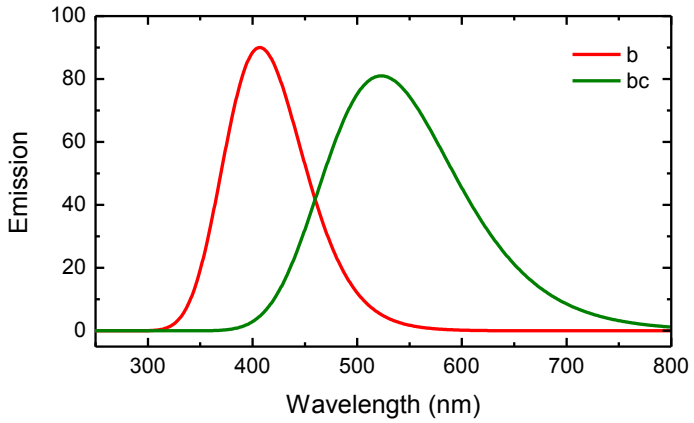

Figure 7: Calculated emission spectra of **b** and **bc.**

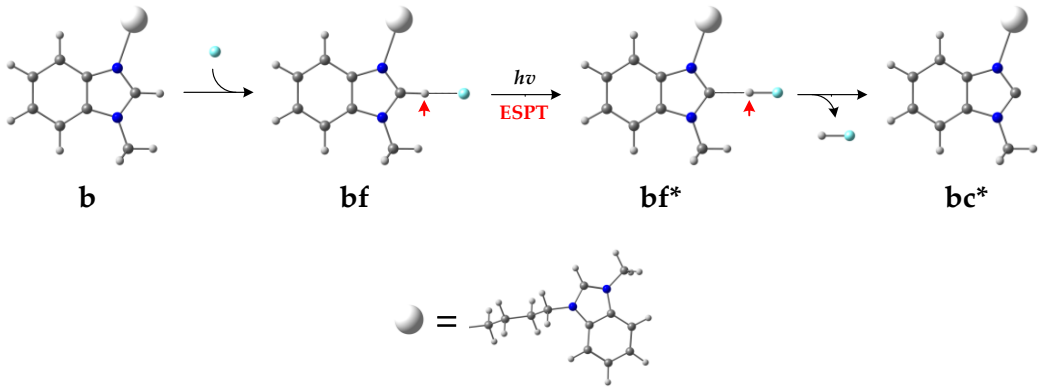

Figure 8: Sensing mechanism for the chemosensor **b** for fluoride anion**.**

4. Conclusion

In summary, we have designed a fluoride chemosensor based on C–H•••F H-bond interaction. The fluoride-sensing mechanism of the chemosensor was described detailedly

by the DFT/TDDFT calculations. The results of geometry optimization showed that the chemosensor-fluoride complex had very different structures in S_0 and S_1 states and there could be an ESPT process. The ESPT process was further confirmed through elucidation of the PES across the reaction coordinate. The calculated data of frontier orbitals and vertical transition energies was used to explain the difference in the chemosensor's fluorescent spectra before and after adding fluoride anions. Due to the difference of emission band between the chemosensor and its carbene form, the designed chemosensor can be used to sense fluoride anion by monitoring the changes in its fluorescence spectrum.

Acknowledgments

This research was financed by the National Natural Science Foundation of China (Nos. 11247281), and Excellent Youth Fund of Hebei Province Department of Education (Y2012010). We also thank Dalian Branch of Supercomputing Center of Chinese Academy of Sciences for computing support.

References

[1] W. L. Jorgensen and J. D. Madura, Temperature and size dependence for Monte Carlo simulations of TIP4P water, Mol. Phys., 56 (1985), 1381.

[2] D. M. Standley, A. R. Kinjo, K. Kinoshita and H. Nakamura, Protein structure databases with new web services for structural biology and biomedical research, Brief. Bioinform., 9 (2008), 276–285.

[3] S. G. Gregory, K. F. Barlow, K. E. McLay, R. Kaul, D. Swarbreck, A. Dunham, C. E. Scott, K. L. Howe, K. Woodfine, C. C. A. Spencer, M. C. Jones, C. Gillson, S. Searle, Y. Zhou, F. Kokocinski, L. McDonald, R. Evans, K. Phillips, A. Atkinson, R. Cooper, C. Jones, R. E. Hall, T. D. Andrews, C. Lloyd, R. Ainscough, J. P. Almeida, K. D. Ambrose, F. Anderson, R. W. Andrew, R. I. S. Ashwell, K. Aubin, A. K. Babbage, C. L. Bagguley, J. Bailey, H. Beasley, G. Bethel, C. P. Bird, S. Bray-Allen, J. Y. Brown, A. J. Brown, D. Buckley, J. Burton, J. Bye, C. Carder, J. C. Chapman, S. Y. Clark, G. Clarke, C. Clee, V. Cobley, R. E. Collier, N. Corby, G. J. Coville, J. Davies, R. Deadman, M. Dunn, M. Earthrowl, A. G. Ellington, H. Errington, A. Frankish, J. Frankland, L. French, P. Garner, J. Garnett, L. Gay, M. R. J. Ghori, R. Gibson, L. M. Gilby, W. Gillett, R. J. Glithero, D. V. Grafham, C. Griffiths, S. Griffiths-Jones, R. Grocock, S. Hammond, E. S. I. Harrison, E. Hart, E. Haugen, P. D. Heath, S. Holmes, K. Holt, P. J. Howden, A. R. Hunt, S. E. Hunt, G. Hunter, J. Isherwood, R. James, C. Johnson, D. Johnson, A. Joy, M. Kay, J. K. Kershaw, M. Kibukawa, A. M. Kimberley, A. King, A. J. Knights, H. Lad, G. Laird, S. Lawlor, D. A. Leongamornlert, D. M. Lloyd, J. Loveland, J. Lovell, M. J. Lush, R. Lyne, S. Martin, M.

Mashreghi-Mohammadi, L. Matthews, N. S. W. Matthews, S. McLaren, S. Milne, S. Mistry, M. J. F. M oore, T. Nickerson, C. N. O'Dell, K. Oliver, A. Palmeiri, S. A. Palmer, A. Parker, D. Patel, A. V. Pearce, A. I. Peck, S. Pelan, K. Phelps, B. J. Phillimore, R. Plumb, J. Rajan, C. Raymond, G. Rouse, C. Saenphimmachak, H. K. Sehra, E. Sheridan, R. Shownkeen, S. Sims, C. D. Skuce, M. Smith, C. Steward, S. Subramanian, N. Sycamore, A. Tracey, A. Tromans, Z. Van Helmond, M. Wall, J. M. Wallis, S. White, S. L. Whitehead, J. E. Wilkinson, D. L. Willey, H. Williams, L. Wilming, P. W. Wray, Z. Wu, A. Coulson, M. Vaudin, J. E. Sulston, R. Durbin, T. Hubbard, R. Wooster, I. Dunham, N. P. Carter, G. McVean, M. T. Ross, J. Harrow, M. V. Olson, S. Beck, J. Rogers and D. R. Bentley, The DNA sequence and biological annotation of human chromosome 1, Nature, 441 (2006), 315–321.

[4] E. Arunan, G. R. Desiraju, R. A. Klein, J. Sadlej, S. Scheiner, I. Alkorta, D. C. Clary, R. H. Crabtree, J. J. Dannenberg, P. Hobza, H. G. Kjaergaard, A. C. Legon, B. Mennucci and D. J. Nesbitt, Definition of the hydrogen bond (IUPAC Recommendations 2011), Pure Appl. Chem., 83 (2011), 1637–1641.

[5] G. A. Jeffrey, An introduction to hydrogen bonding, Oxford University Press, New York, 1997.

[6] G. R. Desiraju and T. Steiner, The weak hydrogen bond, Oxford University Press, Oxford, 1999.

[7] S. Scheiner, Hydrogen bonding, Oxford University Press, New York, 1997.

[8] A. E. Reed, L. A. Curtiss and F. Weinhold, Intermolecular interactions from a natural bond orbital, donor-acceptor viewpoint, Chem. Rev., 88 (1988), 899–926.

[9] K. L. Kirk, Biochemistry of the halogens and inorganic halides, Plenum Press, New York, 1991.

[10] M. Kleerekoper, The role of fluoride in the prevention of osteoporosis, Endocrin. Metab. Clin. North Am., 27 (1998), 441–452.

[11] K. M. K. Swamy, Y. J. Lee, H. N. Lee, J. Chun, Y. Kim, S.-J. Kim and J. Yoon, A new fluorescein derivative bearing a boronic acid group as a fluorescent chemosensor for fluoride ion, J. Org. Chem., 71 (2006), 8626–8628.

[12] R. P. Swatloski, J. D. Holbrey and R. D. Rogers. Ionic liquids are not always green: hydrolysis of 1-butyl-3-methylimidazolium hexafluorophosphate, Green Chem., 5 (2003), 361–363

[13] V. Amendola, M. Boiocchi, L. Fabbrizzi and N. Fusco, Putting the anion into the cage – fluoride inclusion in the smallest trisimidazolium macrotricycle, Eur. J. Org. Chem., 2011 (2011), 6434–6444.

[14] M. Cametti, A. Dalla Cort, L. Mandolini, M. Nissinen and K. Rissanen, Specific recognition of fluoride anion using a metallamacrocycle incorporating a uranyl-salen unit, New J. Chem., 32 (2008), 1113–1116.

[15] Z. Xu, N. J. Singh, S. K. Kim, D. R. Spring, K. S. Kim and J. Yoon, Induction-driven stabilization of the anion–π interaction in electron-rich aromatics as the key to fluoride inclusion in imidazolium-cage receptors, Chem.–Eur. J., 17 (2011), 1163–1170.

[16] Z. Xu, S. K. Kim, S. J. Han, C. Lee, G. Kociok-Kohn, T. D. James and J. Yoon, Ratiometric fluorescence sensing of fluoride ions by an asymmetric bidentate receptor containing a boronic acid and imidazolium group, Eur. J. Org. Chem., 2009 (2009), 3058–3065.

[17] G.-J. Zhao and K.-L. Han, Hydrogen bonding in the electronic excited state, Acc. Chem. Res., 45 (2012), 404–413.

[18] G.-J. Zhao and K.-L. Han, Site-specific solvation of the photoexcited protochlorophyllide a in methanol: formation of the hydrogen-bonded intermediate state induced by hydrogen-bond strengthening, Biophys. J., 94 (2008), 38–46.

[19] G.-J. Zhao, J.-Y. Liu, L.-C. Zhou and K.-L. Han, Site-selective photoinduced electron transfer from alcoholic solvents to the chromophore facilitated by hydrogen bonding: a new fluorescence quenching mechanism, J. Phys. Chem. B, 111 (2007), 8940–8945.

[20] L. Liu, N. Zhao and O. A. Scherman, Ionic liquids as novel guests for cucurbit[6]uril in neutral water, Chem. Commun. 9 (2008), 1070–1072.

[21] J. M. Obliosca, S. D. Arco and M. H. Huang, Synthesis and optical properties of 1-alkyl-3-methylimidazolium lauryl sulfate ionic liquids, J. Fluoresc., 17 (2007), 613–618.

[22] I. Krossing, J. M. Slattery, C. Daguenet, P. J. Dyson, A. Oleinikova and H. Weingärtner, Why are ionic liquids liquid? A simple explanation based on lattice and solvation energies, J. Am. Chem. Soc., 128 (2006), 13427–13434.

[23] I. Billard, G. Moutiers, A. Labet, A. El Azzi, C. Gaillard, C. Mariet and K. Lutzenkirchen, Stability of divalent europium in an ionic liquid: spectroscopic investigations in 1-methyl-3- butylimidazolium hexafluorophosphate Inorg. Chem., 42 (2003), 1726–1733.

[24] C. R. Wade, A. E. J. Broomsgrove, S. Aldridge and F. P. Gabbai, Fluoride ion complexation and sensing using organoboron compounds, Chem. Rev., 110 (2010), 3958–3984.

[25] T. W. Hudnall, C.-W. Chiu and F. P. Gabbai, Fluoride ion recognition by chelating and cationic boranes, Acc. Chem. Res., 42 (2009), 388–397.

[26] F. Neese, ORCA—an ab initio, density functional and semiempirical program package, 2008, http://www.thch.uni-bonn.de/tc/orca/.

[27] A. D. Becke, Density-functional thermochemistry. III. The role of exact exchange, J. Chem. Phys., 98 (1993) 5648–5652.

[28] P. A. Dirac, Quantum mechanics of many-electron systems, Proc, R. Soc. Lond. Ser. A, 123 (1929), 714–733.

[29] S. H. Vosko, L. Wilk and M. Nusair, Accurate spin-dependent electron liquid correlation energies for local spin density calculations: a critical analysis, Can. J. Phys., 58 (1980), 1200–1211.

[30] A. D. Becke, Density-functional exchange-energy approximation with correct asymptotic behavior, Phys. Rev. A, 38 (1988), 3098–3100.

[31] G.-Y. Li, P. Song and G.-Z. He, TDDFT study on different sensing mechanisms of similar cyanide sensors based on michael addition reaction, Chin. J. Chem. Phys., 24 (2011), 305-310.

[32] G.-Y. Li and T.-S. Chu, TD-DFT study on fluoride-sensing mechanism of 2-(2′-phenylureaphenyl) benzoxazole: the way to inhibit the ESIPT process, Phys. Chem. Chem. Phys., 13 (2011), 20766–20771.

[33] O. Treutler and R. J. Ahlrichs, Efficient molecular numerical integration schemes, Chem. Phys., 102 (1995), 346–356.

[34] A. Klamt, G. Schüürmann, COSMO: a new approach to dielectric screening in solvents with explicit expressions for the screening energy and its gradient, J. Chem. Soc. Perkin. Trans. 2, 5 (1993), 799–805.

[35] D. R. Lide, CRC Handbook of Chemistry and Physics, 84th ed., CRC Press, Cleveland, 2004.

[36] K. J. Cahill and R. P. Johnson, Beyond frontier molecular orbital theory: a systematic electron transfer model (ETM) for polar bimolecular organic reactions, J. Org. Chem., asap, doi: 10.1021/jo301731v.